

## 3D GPR reveals complex internal structure of Pleistocene oolitic sandbar

MARK GRASMUECK and RALF WEGER, University of Miami, Florida, U.S.

Active oolitic sandbars like those in the Bahamas (Figure 1) exhibit complex internal architecture with a multitude of stacked sedimentary structures. Ooids are round, carbonate-coated grains that form in tropical climates. The internal anatomy of carbonate sandbars is often too complex to be captured in one- and two-dimensional data. Outcrops, cores, and 2D geophysical profiles provide a limited vertical view of the geologic record. Depositional processes are confined to the momentary subhorizontal boundary surface between sediment and water or air. Vertical 2D views limit the visibility of features developed on subhorizontal surfaces, making interpretation of 3D internal anatomy and reconstruction of related depositional parameters difficult. Closely spaced 3D data are needed to accurately map sedimentary structures and improve fluid flow modeling used in water and hydrocarbon resource management. 3D reflection seismic imaging has successfully been used to delineate oolitic bars in subsurface oil fields. Unfortunately, seismic resolution that resolves beds in the order of 10 m thick, fails to image the detailed internal anatomy of oolitic sand bodies.

GPR, however, has emerged as a useful tool for shallow imaging of outcropping sedimentary deposits. Bristow et al. (2000) measured a grid of 2D GPR profiles over a linear sand dune in Namibia and found that older simplistic depositional models of linear sand dunes had to be revised. Three-dimensional GPR imaging has also been shown to give insight into the internal anatomy of fluvial deposits (Beres et al., 1999; Corbeau et al., 2001) and other geomorphic settings (Junck and Jol, 2000). Due to surveying speed limitations, compromises usually have to be made with respect to survey size and spatial resolution. As a result, horizontal slices usually contain interpolation artifacts and do not show the full detail of subsurface geometry, especially for randomly dipping features.

This study combines outcrop information from the Miami Oolite, a Pleistocene limestone formation that forms the bedrock of the greater Miami area, with a 24 x 46 x 7 meter 3D 100-MHz GPR data cube sampled at 0.6 ns. This corresponds to 0.024 m at a velocity of 0.08 m/s. The 100 MHz wavelength is 0.8 m. The acquired high-density grid spacing of 0.1 x 0.2 m permits analysis of depositional environments in horizontal slices of unprecedented detail.

**The Miami Oolite: Relict Pleistocene tidal and barrier bars.** During the Pleistocene (120 000 years ago), the Miami area looked very similar to modern day Joulters Cays in the Bahamas (Figure 2). The oolitic facies (Figure 3) of the Miami Limestone consists of a southwest-trending ridge extending more than 50 km south from Miami. The ridge was created during an interglacial sea level highstand as much as 6 m above today's level. Much original morphology has been preserved. General features of tidal bars are evident on topographic maps. The 10-km wide oolitic ridge consists of a series of slight topographic highs interpreted as tidal bar areas, separated by narrow elongated sinuous low areas

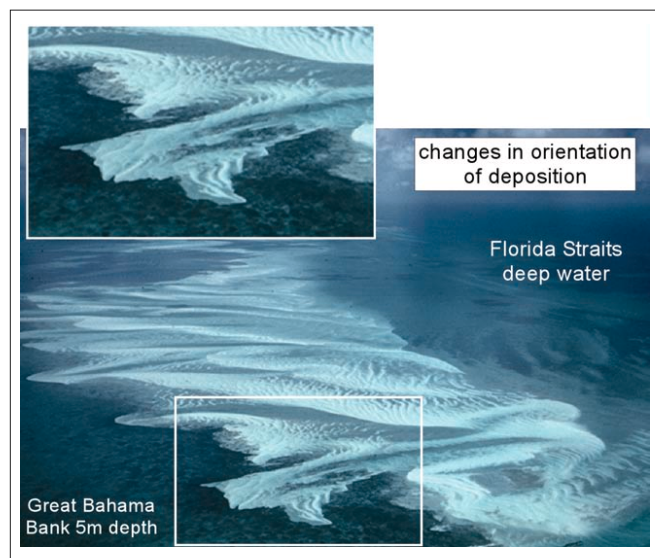


Figure 1. Oblique aerial photograph of complex and very dynamic oolite tidal bars and channels on the western edge of Great Bahama Bank. Light colors = white oolitic sand bars just under the water surface. Darker areas = tidal channels 2-4 m deep. Zoomed in is a spillover lobe (Ball, 1967) of oolitic sands created by tidal flood currents. Sandwaves with 20-50 cm height are superimposed on the tidal bars. (Photograph courtesy SEPM, Marine Carbonates I: Models, seismic response and Quaternary of Florida-Bahamas, CD No. 1.)

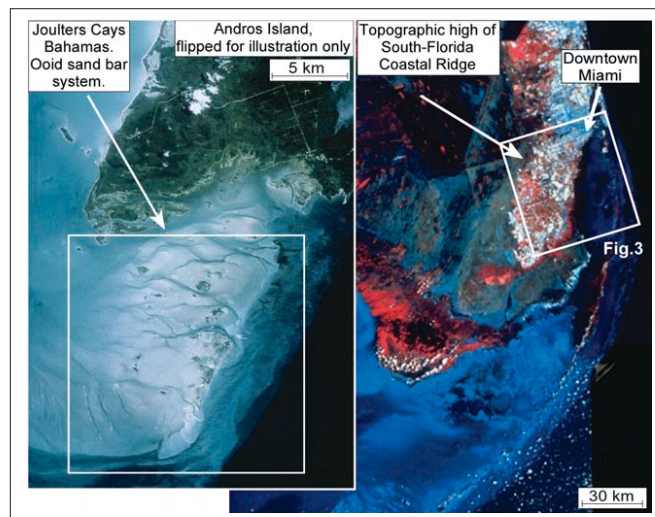


Figure 2. Satellite images of South Florida and Joulters Cays, Bahamas, are compared to illustrate the similarity in morphology and general outline between ancient and modern oolitic sand bodies. (Photographs courtesy SEPM, Marine Carbonates I: Models, seismic response and Quaternary of Florida-Bahamas, CD No. 1.)

interpreted as relict tidal channels. Halley et al. (1977) delineated an oolitic barrier bar in front of the shoals. The bar is 0.8 km wide and 35 km long, leaving the southern tidal bars of the Miami oolitic ridge unprotected from the open ocean

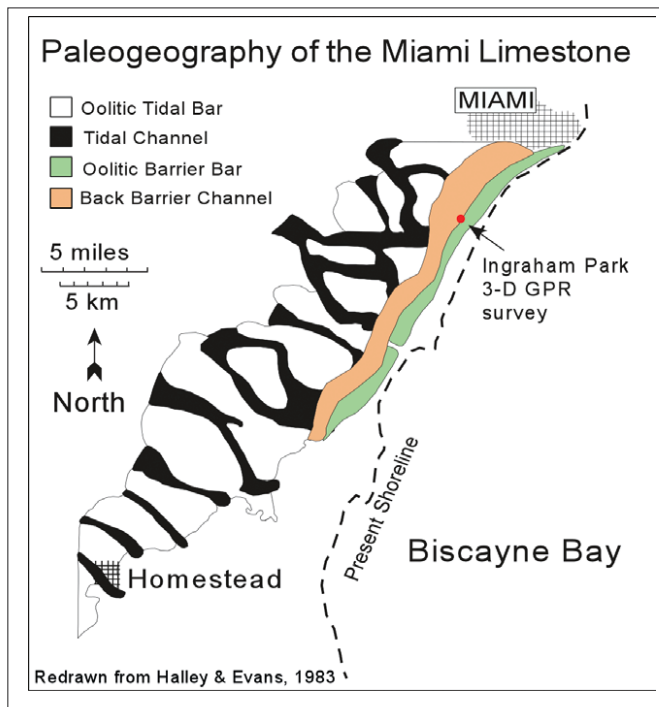


Figure 3. Paleogeographic reconstruction of Pleistocene oolitic tidal bar and barrier bar complex based primarily on present-day topography.

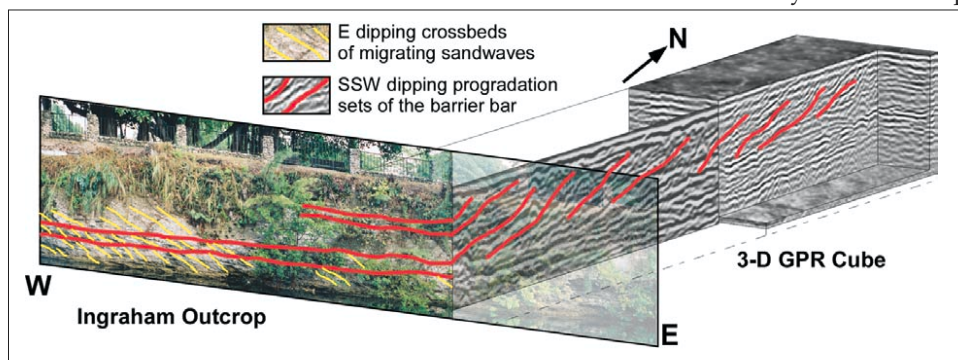


Figure 4. Composite display of Ingraham outcrop, 3D GPR data cube, and 29-m GPR profile linking the outcrop to the data cube. SSW-dipping reflectors (red) in GPR data can be correlated with the set boundaries of centimeter scale east dipping cross-bedding (yellow) in the outcrop.

at time of deposition.

The 3D GPR survey area is on the Miami Oolite barrier bar. Cross-bedded oolitic grainstones and burrowed peloidal-oid grainstones outcrop 30 m south (Figure 4). The cross-bedded lithofacies consists of regularly spaced, coarsening upward, 1-2 cm thick couplets that are grouped into subhorizontal sets of 0.5-1 m thickness. Average dip angle of the cross-bed couplets is 26°. The depositional environment has been interpreted as alternating high-energy ooid sand deposition and low-energy periods of bioturbation. Mostly eastward-dipping cross-beds suggest eastward migration of decimeter scale sandwaves during high-energy events.

**Technique of high-resolution 3D GPR surveying.** Most subsurface radar reflections are caused by changes in water content. Moisture content in sedimentary rocks is generally controlled by grain size, porosity, and permeability. This makes GPR an ideal tool to image shallow sedimentary bodies. In the Miami Oolite, sedimentary structures are excellently preserved due to selective cementation. GPR does not penetrate saline pore water and is therefore not

applicable to oolitic bars still saturated with marine water.

A 3D GPR campaign normally starts with a reconnaissance survey of 2D profiles to get an idea of GPR performance and subsurface geology. GPR data are acquired by moving the transmitter and receiver antennas over the area of interest. Based on the 2D survey, a field of interest is chosen to perform 3D surveying. A 3D GPR survey is essentially equivalent to single-channel 3D seismic data acquisition. Closely spaced cross sections are fused into a continuous 3D data volume. The spatially unaliased sampling of steep-dipping features and diffractions with 100-MHz GPR antennas requires line spacing as small as 10 or 20 cm.

For efficient surveying of tennis court size and larger areas, continuous antenna movement and centimeter-precise positioning of the antennas at all times are required. Commercially available 3D GPR systems have been developed for detection of concrete rebars and utilities under smooth and flat surfaces. The antennas are equipped with an odometer wheel rolling over the surface. For geologic applications on natural surfaces, with soil, vegetation, and elevation changes, the survey wheel approach is not precise enough. As a result, the sharpness of the resulting 3D data volume decreases. Stepped data acquisition by positioning the antennas manually at every survey point is very slow, but is common practice for small low-resolution surveys. Fast 3D GPR systems suitable for geologic fieldwork exist only as academic prototypes.

The survey area of this study was on a grass field in a public park just above the outcrop in Figure 4. Two individuals completed the Miami Oolite 3D GPR survey in nine hours; 56 000 radar traces were collected with a trace recorded every 0.1 m on 121 parallel north-south lines spaced by 0.2 m. Transmitter and receiver separation was 0.56 m. Data processing included drift correction of onset time, removal of low-period signal offsets by mean filtering, amplitude decay compensation with the same function applied to all

traces and 30-240 MHz bandpass filtering. Profile alignment was adjusted before fusion into the data cube.

Radar velocities for depth estimation were derived from a subset of the 66 CMPs collected on a 4-m grid over the entire survey area. An average velocity of 0.08 m/ns was determined from semblance analysis of the deepest coherent reflections at approximately 150 ns (twt), corresponding to a depth of approximately 6 m.

**3D internal reflectors seen using GPR detect sediment transport direction.** Our GPR survey provides a first ever look at the oolitic carbonate environment in three dimensions. The 3D-rendered data cube reveals generally south-southwest dipping reflectors (Figure 4). This dip direction deviates 90° from the small-scale cross-bedding observed in the nearby outcrop. The GPR reflectors can be correlated to bounding surfaces between cross-bedded sets of 0.5-1 m thickness. Gonzalez and Eberli (1997) have previously documented large-scale prograding foresets superimposed by small-scale sinuous and linear ripples with dip directions deviating by as much as 90° on an active Bahamian oolitic shoal. The large-scale dip observed in the data set indicates



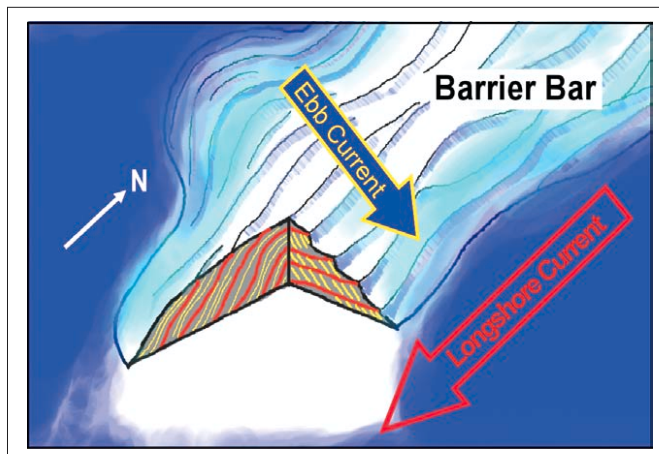


**Figure 5.** Conceptual model illustrating the growth of the Miami oolitic barrier bar. The set boundaries (red) recently detected with 3D GPR imaging indicate southward progradation due to longshore currents. The eastward-dipping smaller scale cross-beds (yellow) in the outcrop are the internal structures of N-S trending sandwaves created by the ebb tidal current flowing over the prograding end of the barrier bar.

different levels of the 3D data volume show spatial variations of sedimentary patterns that can be related to changes in depositional environments. These environmental changes might be of local nature or are related to overall changes affecting the entire Miami oolitic system.

**Ancient sand wave patterns revealed.** At a depth of 6 m, a 1-m thick sedimentary unit with internal reflections dipping at an angle of 3-5° overlies the base reflector that dips at 2° to the south. In the horizontal view of Figure 7a, the reflections are concave to the south, which can be interpreted as draping of sediments by longshore currents into the pre-existing topography of the marine basement in 5-10 m water depth. At the level of slice B (Figure 7), topography had been flattened out. A linear 10-m wide N-S channel developed and was filled with N-S trending sand waves indicated by parallel lineations within the channel. In the northwestern corner, horn-shaped patterns similar to the parabolic ends of spillover lobes in Figure 1 are visible. A wedge-shaped high (Figure 7c) developed, showing a “wormy” internal character and diffraction patterns visible on the cross section in Figure 6. The original sedimentary layering appears

to have been destroyed by burrowing organisms. The settling of burrowers indicates stable and fairly low-energy conditions. Slice 7d illustrates a drastic change in depositional environment. Reflectors that are dipping at 5-7° with continuity of 14-28 m delineating packages of 0.5-1 m thicknesses are interpreted as rapid progradation of the barrier bar. As previously discussed (Figures 4 and 5), this process probably filled most of the available accommodation space, causing approximately 3-m decrease of water depth.

The dense grid spacing (0.1 3 0.2 m) enables detection of subtle sedimentary patterns on time slices. For example, lineations indicative of N-S trending sand-waves are visible on horizontal slices (Figure 7b). Decimation of our data to simulate common grid spacings of “3D” GPR surveys (Figure 8) illustrates the loss of these fine-scale lineation patterns. The successful imaging of submeter-scale sedimentary structures, interference patterns from centimeter scale cross-bedding and diffractions is dependent on a

horizontal grid spacing that approaches a quarter of a wavelength. For 100 MHz and a velocity of 0.08 m/ns, this is 0.2 m, the line spacing of our survey.

It remains to be tested how detailed velocity analysis, 3D depth migration, and volume-based extraction of wavelet attributes will further enhance the ability to image the complexities of the internal anatomy of oolitic sandbars. Future 3D GPR surveys in other locations of the Miami Oolite will further establish the variations in spatial relationships on a larger scale. Eventually, knowledge from this case study can be applied to oolitic reservoirs.

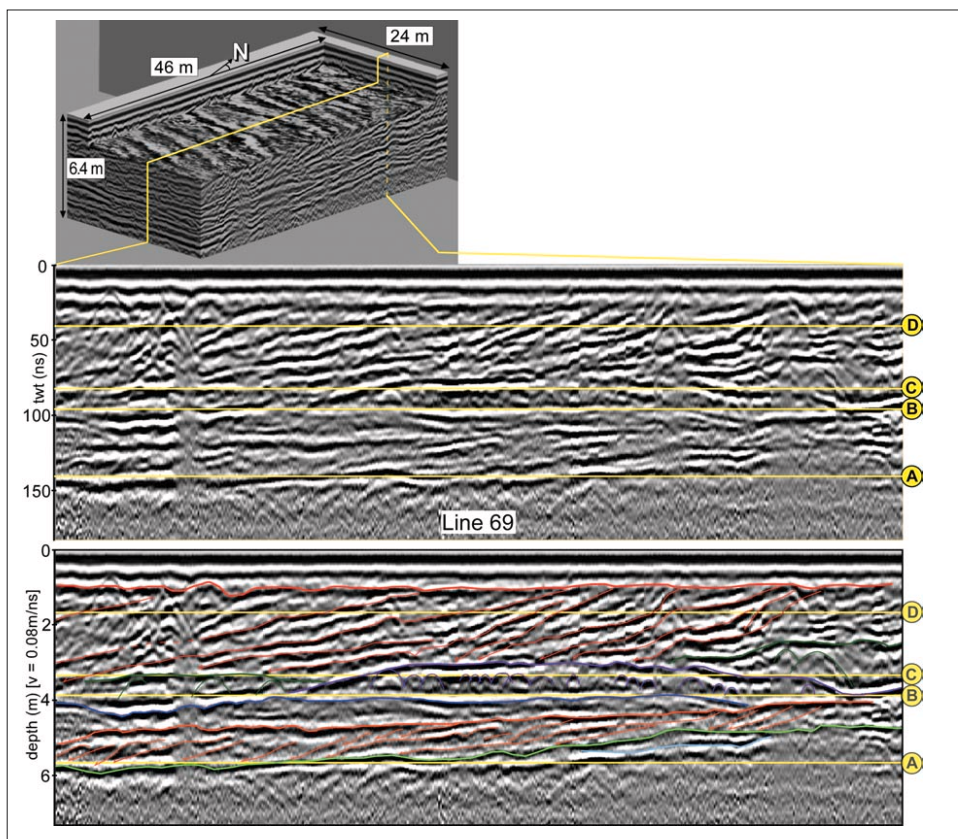


**Figure 6.** 100-MHz 3D GPR data cube and a vertical cross section at Ingraham Park. The cube’s horizontal cutout shows strikelines of SSW-dipping progradational set boundaries. A, B, C, and D denote depths of horizontal slices in Figure 7. Line drawing depicts sedimentary units with different character.

a sediment transport direction perpendicular to the one visible at the outcrop. The SSW dip is parallel to the main growth direction of the barrier bar and confirms the geomorphological observations by Halley et al. (1977). Smaller-scale cross-bedding observed in the outcrop suggests seaward and landward direction of tidal and wave processes, superimposed on the larger-scale progradation of barrier bar sets (Figure 5).

Detailed stratigraphic analysis of the 3D GPR volume (Figures 6 and 7) reveals sedimentary units with different character. Vertical sections combined with map views from



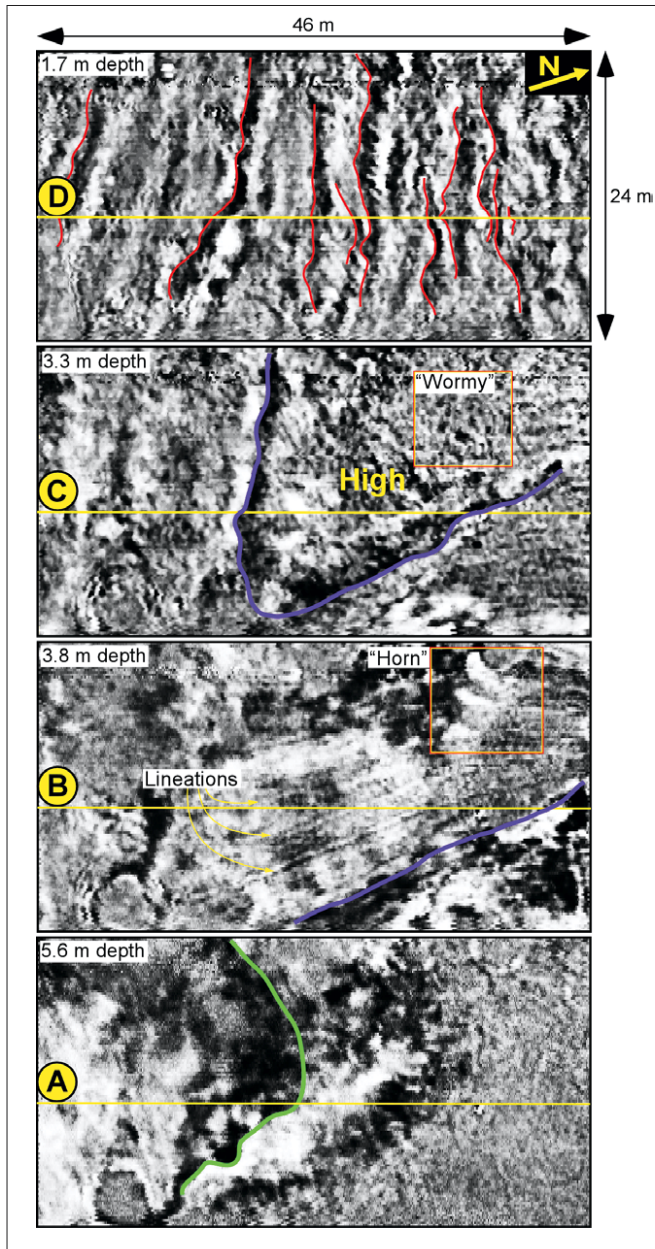


**Figure 7.** Horizontal slices through 3D GPR volume acquired at Ingraham Park. The geometries and patterns on the slices represent changing depositional environments. Colors of features interpreted on slices match colors in Figure 6.

**Conclusion.** This successful 3D GPR survey in an oolitic limestone environment offers new insight into the spatial distribution of sedimentary features. It was possible to image the internal architecture of a complex oolitic sandbar system on a submeter scale and to confirm relationships that exist between decimeter-scale sandwaves and the prograding barrier bar. Only the dense grid spacing used for this survey provided the necessary basis for accurate description of 3D internal anatomy and paleoenvironmental parameters such as dominant wave and current direction. Such reconstruction of depositional environment would not have been possible with commonly used 0.5-1 m line separation (Figure 8).

3D GPR data volumes, together with the 3D technologies from seismic exploration, will enable unprecedented quantification of internal anatomy of sedimentary bodies, filling the scale gap between borehole and seismic infor-

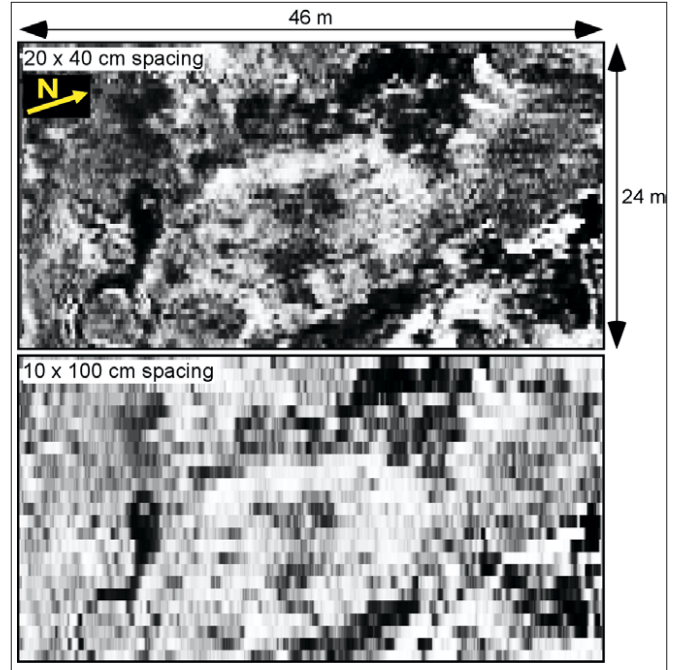


**Figure 8.** Simulation of coarser-acquisition grid spacing (0.2 × 0.4 m and 0.1 × 1.0 m) demonstrates the loss of detail visible on horizontal slices. Compared to the original (0.1 × 0.2 m, Figure 7b), which clearly images circular diffraction patterns and N-S oriented sand-wave lineations, the subsampled slices obscure or do not resolve features indicative of internal sedimentary structures.

mation. Advances in 3D GPR data acquisition technology are needed to make such surveys commercially viable and not only a matter of academic research.

Movies from the 3D GPR cube are viewable at <http://mgs.rsmas.miami.edu/groups/csl/gpr/>.

**Suggested reading.** “Carbonate sand bodies of Florida and the Bahamas” by Ball (*Journal of Sedimentary Petrology*, 1977). “Using two- and three-dimensional georadar methods to characterize glaciofluvial architecture” by Beres et al. (*Sedimentary Geology*, 1999). “The sedimentary structure of linear sand dunes” by Bristow et al. (*Nature*, 2000). “Detailed internal architecture of a fluvial channel sandstone determined from outcrop, cores, and 3D ground-penetrating radar; example from the Middle Cretaceous Ferron Sandstone, east-central Utah” by Corbeau et al. (*AAPG Bulletin*, 2001). “Sediment transport and bedforms in a carbonate tidal inlet; Lee Stocking Island, Exumas, Bahamas” by Gonzalez and Eberli (*Sedimentology*, 1997). “3D ground-penetrating radar applied to fracture imaging in gneiss” by Grasmueck (*GEOPHYSICS*, 1996). “Pleistocene barrier bar seaward of ooid shoal complex near Miami, Florida” by Halley et al. (*AAPG Bulletin*, 1977). “Three-dimensional investigation of geomorphic environments using ground-penetrating radar” by Junck and Jol (*SPIE Proceedings Series*, 2000). “Semiautomated georadar data acquisition in three dimensions” by Lehmann and Green (*GEOPHYSICS*, 1999). “Ground-penetrating radar: A near-face experience from Washington County, Arkansas” by Liner and Liner (*TLE*, 1995). **TJE**

*Acknowledgments:* We thank the Rosenstiel School of Marine and Atmospheric Science, Division of Marine Geology and Geophysics, for its support with personnel and facilities. Furthermore, we greatly appreciate the advice and suggestions offered by members of the Comparative Sedimentology Laboratory.

Corresponding author: [mgrasmueck@rsmas.miami.edu](mailto:mgrasmueck@rsmas.miami.edu)